A&A manuscript no.
(will be inserted by hand later)

Your thesaurus codes are:
08.16.7, PSR J0537−6910, 03.09.1

ASTRONOMY AND ASTROPHYSICS

Search for the optical counterpart of the 16ms X-ray pulsar in the LMC ⋆

R. P. Mignani[1], L. Pulone[2], G. Marconi[2], G. Iannicola[2] and P.A. Caraveo[3,4]

[1] ESA/ST-ECF, Karl-Schwarzschild-Str.2 D-85740 Garching, Germany - email: rmignani@eso.org
[2] Osservatorio Astronomico di Roma, Via di Frascati 33, I-00040 Monte Porzio Catone, Italy
[3] Istituto di Fisica Cosmica "G. Occhialini", CNR, Via Bassini 15, I-20133-Milan, Italy
[4] Istituto Astronomico, Via Lancisi 29, I-00161-Rome, Italy

Received 19 August 1999; accepted 23 November 1999

Abstract. The 16ms X-ray pulsar PSR J0537−6910 in SNR N157B is the fastest known isolated (non-recycled) pulsar and, with a rotational energy loss $\dot{E} \sim 4.8 \times 10^{38}$ erg s^{-1}, is the most energetic (together with the Crab). Here we report the results of optical observations of the field, recently performed with the SUSI2 camera of the NTT. Few objects are observed inside the $\simeq 3''$ X-ray error circle but none of them can be convincingly associated to the pulsar, which appears undetected down to $V \sim 23.4$. With a corresponding optical luminosity $L_{\rm opt} \leq 1.3 \times 10^{33}$ erg s^{-1}, PSR J0537−6910 is, at best, comparable to the other very young pulsars Crab and PSR B0540−69.

Key words: Stars: pulsars: individual: PSR J0537−6910 Instrumentation: detectors

1. Introduction

PSR J0537−6910 is a young, fast, X-ray pulsar, recently discovered at the center of the LMC supernova remnant N157B, close to the 30 Doradus star forming region. N157B belongs to the class of the so called Crab-like supernova remnants, or plerions, characterized by non-thermal spectra and a centrally-filled radio/X-ray morphology probably due to the presence of a synchrotron nebula powered by the relativistic wind from a young, energetic, pulsar. Apart from the Crab Nebula, so far only three other plerions were known to host pulsars, namely: SNR0540−69 (PSR B0540−69), also belonging to 30 Doradus complex and located $15'$ from N157B, MSH−15-52 (PSR B1509−58) and G11.2−0.3 (PSR J1811−1926). Thus, with the detection of PSR J0537−6910, N157B represents the fifth case of a plerion/pulsar association.
Pulsed X-ray emission at 16 ms was serendipitously discovered during a RXTE/PCA observation towards 30 Doradus (Marshall et al. 1998). Soon after, the pulsation was detected in archived 1993 ASCA/GIS data and additional confirmations came from BeppoSAX (Cusumano et al. 1998). PSR J0537−6910 takes over the Crab (33 ms) as the fastest "classical" (i.e. not spun up by matter accretion from a companion star) pulsar.
The pulsar was identified in the ASCA/GIS with a X-ray source detected at the center of N157B and resolved in a point-like component (the pulsar and, probably, its associated synchrotron nebula) plus an elongated feature, the origin of which is still uncertain. In both RXTE and ASCA data, the pulse profile appears characterized by a sharp (~ 1.7 ms FWHM) symmetric peak, which shows no obvious evolution during the time interval between ASCA and RXTE observations (3.5 yrs). The period derivative of the pulsar ($\dot{P} \simeq 5 \times 10^{-14}$ s s^{-1}), obtained from the comparison of multi-epoch timing (Marshall et al. 1998; Cusumano et al. 1998), gives a spindown age of $\approx 5\,000$ yrs), similar to the age of the remnant estimated by Wang & Gotthelf (1998a), a magnetic field of $\approx 10^{12}$ G, typical for a pulsar this young, and a rotational energy loss $\dot{E} \sim 4.8 \times 10^{38}$ ergs s^{-1}. Substantially the same results were obtained from the timing analysis of ROSAT/HRI data (Wang & Gotthelf 1998b).
In radio, PSR J0537−6910 has been observed between June and August 1998 using the 64m radio telescope in Parkes but it has not been detected down to an upper limit of $F_{14.\rm GHz} \sim 0.04$ mJy (Crawford et al. 1998). Although not really compelling, the present upper limit suggests that PSR J0537−6910 is weaker in radio than both the Crab pulsar and PSR B0540−69.

2. Optical observations

While in radio PSR J0537−6910 is an elusive target, in the optical domain the situation appears more promising. Up to now, three of the five pulsars younger than 10 000 yrs have been certainly identified in the optical (Mignani 1998), where they channel through magnetospheric emission $\sim 10^{-5}-10^{-6}$ of their rotational energy output. Since

Send offprint requests to: R.P. Mignani (rmignani@eso.org)
⋆ Based on observations collected at the European Southern Observatory, La Silla, Chile

PSR J0537−6910 is very young ($\simeq 5\,000$ yrs) and, with the Crab, it has the highest $\dot{E}$, it is natural to assume that also in this case a significant amount of the rotating power be radiated in the optical. However, given the uncertain dependance of the optical luminosity vs. the pulsar parameters, it is difficult to make a prediction on the actual magnitude of PSR J0537−6910. A possible estimate can be obtained by a straight scaling of the Pacini's relation (see e.g. Pacini & Salvati 1987) i.e. neglecting the dependance of the pulsar luminosity on its unknown optical duty cycle. This would yield $V \simeq 24.6$, after correcting for the interstellar absorption $A_{\rm V} \sim 1.3$, estimated applying the relation of Fitzpatrick (1986) with an $N_{\rm H} \sim 10^{22}$ cm^{-2}, measured by the X-ray spectral fittings (Wang & Gotthelf 1998a). However, we note that the other young ($\sim 2\,000$ yrs) LMC pulsar, PSR B0540−69, with a factor 3 smaller $\dot{E}$, has a magnitude $V = 22.4$ with an $A_{\rm V} \sim 0.6$ (Caraveo et al. 1992).

Although PSR J0537−6910 is still undetectable in radio, its detection in ROSAT/HRI data (Wang & Gotthelf 1998b) reduces significantly its position uncertainty down to $\pm\ 3''$and prompts the search for its optical counterpart. The scientific case appears similar to the one of PSR B0540−69, also discovered as a pulsating X-ray source (Seward et al. 1984), also embedded in a supernova remnant (SNR0540−69) and tentatively identified in the optical without the aid of a reference radio position (Caraveo et al. 1992).

In the following, we describe the results of the first deep imaging of the field of PSR J0537−6910, performed with the ESO/NTT.

2.1. The data set

The field of PSR J0537−6910 has been observed in three different runs between September and November 1998 from the European Southern Observatory (La Silla). The observations have been performed in visitor mode with the NTT, equipped with the second generation of the SUperb Seeing Imager camera (SUSI2). The camera is a CCD with a field of view of $5\farcm5 \times 5\farcm5$, split in two chips, and a projected 2×2 binned pixel size of $0\farcs16$. The two CCD chips are physically separated by a gap $\simeq 100$ pixels in size, corresponding to an effective sky masking of $\simeq 8''$.

Images were obtained in different wide-band filters (B, V, I) and in the narrow-band H_α, with the available data set summarized in Table 1.

After the basic reduction steps (bias subtraction, flat-field correction, etc.), single exposures have been combined and cleaned from cosmic ray hits by frame-to-frame comparison. The frames taken through the same filter have been registered with respect to each other and combined through a median filter. The conversion from instrumental magnitudes to the Johnson standard system was obtained using a set of primary calibrators from Landolt fields observed at different airmasses during each night. The formal errors in the zero point of the calibration curves are 0.04 magnitudes in V and B, and 0.03 in I.

Astrometry on the field has been computed using as a reference the coordinates and positions of a set of stars extracted from the USNO catalogue. Then the sky-to-pixel coordinate transformation has been computed using the ASTROM software (Wallace 1990), yielding a final accuracy of $0\farcs4$ on the astrometric fit.

Fig. 1 shows a 1200s exposure H_α image of the 30 Doradus region, obtained through the SUSI2 camera. The solid square ($20'' \times 20''$), located close to the maximum of the emission in the H_α band just at the center of the star forming region, includes the X-ray position of PSR J0537−6910 (Wang & Gotthelf 1998b). A zoomed I-band image of this area is shown in Fig. 2 in negative greyscale.

2.2. Results

Few objects are seen close or within the X-ray error circle of the pulsar (Fig. 2), including the moderately bright ($V \simeq 19$) star #1. However, the crowding of the region, together with the irregular sky background conditions, prompted us to apply automatic object detection routines to search for additional, barely detectable, candidates.

The object search in the X-ray error circle was thus performed using the ROMAFOT package for photometry in crowded fields (Buonanno & Iannicola 1989). The ROMAFOT parameters were tuned to achieve in each filter a conservative $\geq 5\sigma$ object detection above the local background level. A template PSF was obtained by fitting the intensity profiles of some of the brightest, unsaturated, isolated stars in the field with a Moffat function, plus a numerical map of the residual to better take into account the contribution of the stellar wings. To allow for an automatic object matching and make the color-color analysis faster, all the images have been aligned to a common reference frame. As a reference for object detection we have used our I-band image, where the effects of the local absorption are reduced. The master list of objects thus created was then registered on the images taken in B and V filters and used as an input for the fitting procedure. A carefully check by eye has been performed in

Table 1. Summary of the available NTT observations of the PSR J0537−6910 field. Columns list the observing epochs, the imaging device, the filters, the total exposure times in seconds and the average seeing conditions during each observation.

Date	*Detector*	*Filter*	*T(s)*	*Seeing*
Sept 98	SUSI2	V	1800 s	$1\farcs2$
	SUSI2	I	2400 s	$1\farcs0$
	SUSI2	H_α	1200 s	$1''.0$
Oct 98	SUSI2	B	3×500 s	$1\farcs2$
Nov 98	SUSI2	V	2×900 s	$0\farcs8$

Table 2. Observed, not dereddened, magnitudes of the objects observed inside/close to the X-ray error circle. Objects are identified by their labels in Fig. 2. Columns list the V-band magnitudes, and colors. Attached photometric errors are $\simeq 0.02$ mag and $\simeq 0.1$ mag at $V = 18$ and $V = 21$, respectively.

Id	*V*	*B-V*	*V-I*
1	18.8	0.38	0.45
2	21.2	>1.9	0.85
3	20.4	0.40	0.02
4	20.7	>2.4	0.72
5	19.9	0.32	0.11
6	20.5	0.58	-0.70
7	20.0	0.54	1.58
8	19.8	0.72	0.62
9	19.8	0.95	1.11
10	20.8	0.21	0.74
11	20.0	0.35	0.36
12	17.4	0.13	0.27

order to ensure that all the stellar objects found in the I band were successfully fitted in the other images. Apart from the ones labelled in Fig.2, no other candidate optical counterpart to the pulsar has been clearly detected by our procedure. We just report the possible presence in the I-band image of an ~ 22.3 magnitude object (not recognizable in Fig.2), right below the detection threshold and located nearly at the center of the error circle. However, the very low significance of this detection as well as the lack of color information prevent us to assess the nature of this object and to speculate about a possible association with the pulsar.

The properties of objects #1-#12, i.e. their magnitudes and colors ($B-V$ and $V-I$) are summarized in Table 2. According to their colors and brightness, all these objects are likely identified as young massive stars. Fig. 3 shows the color–magnitude (I vs $V-I$) diagram computed for a sample of objects selected in a $\sim 0\farcm5 \times 0\farcm5$ surrounding area (the region marked by the dashed box in Fig. 1), together with the Zero Age Main Sequence track estimated from a suitable chemical composition ($Z = 0.008$, $Y = 0.23$) for the LMC stellar population (Cassisi, private comm.). The objects labelled in Fig. 2 and listed in Table 2 have been marked by open diamonds. Although broadened by the interstellar absorption and shifted redward by the differential reddening, the color–magnitude diagram (CMD) of all the stars is indeed consistent with a young stellar population main sequence. Thus, the optical counterpart of PSR J0537−6910 is probably too faint to be detected against the high background induced by the supernova remnant and the absorption of the embedding HII region. Using the template PSFs computed from each image, artificial stars tests have been run to estimate the V, B, and I magnitude limits of our images. With the flux normalization left as a free parameter, artificial stars have simulated and added to the corresponding images at 100 different positions randomly selected inside the error circle. Thus, the detection algorithm has been run in a loop for the above number of trials, with the flux normalization adjusted to allow for a 3σ detection in each filter. Averaging over the number of trials, we have found 3σ detection limits corresponding (within 0.2 mag) to $B \simeq 23.2$, $V \simeq 23.4$ and $I \simeq 22.4$, which we have taken as an indication of the limiting magnitudes achievable in each band.

3. Conclusions

We have performed deep optical observations to search for the optical counterpart of the isolated X-ray pulsar PSR J0537−6910. However, none of the objects detected close to/inside the X-ray error circle stands out as a convincing candidate. The marginal detection of a $I \sim 22.3$ object at the center of the error circle must be regarded as tentative and is in need of future confirmation. The optical counterpart of PSR J0537−6910 is thus unidentified down to a 3σ limiting magnitude of $\simeq 23.4$ in V. Our result is in agreement with the upper limits recently derived by Gouiffes & Ögelman (1999) on the pulsed optical flux. At the distance of 47 kpc estimated for the host remnant N157B (Gould 1995) and for the assumed interstellar absorption ($A_{\rm V} \simeq 1.3$), our upper limit corresponds to an optical luminosity $L_{\rm opt} \leq 1.3 \times 10^{33}$ erg s^{-1}. This implies that PSR J0537−6910 is, at best, of luminosity comparable to the ones of the Crab and PSR B0540−69, in line with the predictions of Pacini's law. Although interesting, this upper limit is not stringent enough to put strong constraints on the evolution of non-thermal optical emission of young pulsars. Together with the recent upper limit obtained for PSR B1706−44 (Mignani et al. 1999), the measurement of the optical luminosity of PSR J0537−6910 would be crucial to smoothly join the class of the very young ($\simeq 1\,000$ years) and bright objects with the class of older, Vela-like ($\simeq 10\,000$ years) ones, for which the optical output is $\simeq 4$ orders of magnitude lower (Mignani 1998).

As in the case of PSR B0540−69 (Shearer et al. 1994), time-resolved high resolution, imaging, possibly exploiting the more accurate X-ray position available from future Chandra observations, would be the best way to pinpoint and identify the optical counterpart of PSR J0537−6910.

Acknowledgements. We acknowledge the support software provided by the Starlink Project which is funded by the UK SERC. Part of the SUSI2 observations were performed in guaranteed time as part of the agreement between ESO and the Astronomical Observatory of Rome. Last, we would like to thank the anonymous referee for his/her useful comments to the manuscript.

References

Buonanno R., Iannicola G., 1989, PASP 101, 294

Caraveo P.A., Bignami G.F., Mereghetti S., Mombelli M., 1992, ApJ 395, L103
Crawford F., Kaspi V.M., Manchester R.N., et al., 1998, MmSAI 69, 951
Cusumano G., Maccarone M.C., Mineo T., et al., 1998, A&A 333, L55
Fitzpatrick E.L., 1986, AJ 92, 1068
Gouiffes K. & Ögelman H., 1999, Proc. of IAU Colloquium No. 177: PULSAR ASTRONOMY - 2000 and Beyond, M.Kramer, N.Wex and R.Wielebinski, eds. ASP Conference Series - in press
Gould A., 1995, ApJ 452, 189
Marshall F.E., Gotthelf E.V., Zhang W., et al., 1998, ApJ 499, L179
Mignani R., 1998, Proc. of Neutron Stars and Pulsars: Thirty years after the discovery. N. Shibazaki, N. Kawai, S. Shibata, T. Kifune, eds. Universal Academic Press, Frontiers science series n.24, p.335
Mignani R., Caraveo P.A., Bignami G.F., 1999, A&A 343, L5
Pacini S., Salvati M., 1987, ApJ 321, 447
Seward F.D., Harnden F.R., Helfand D.J., 1984, ApJ 287, L19
Shearer A., Redfen M., Pedersen H., et al., 1994, ApJ 423, L51
Wallace P.T., 1990, Starlink User Note 5.11, Rutherford Appleton Laboratory
Wang Q.D., Gotthelf E.V., 1998a, ApJ 494, 623
Wang Q.D., Gotthelf E.V., 1998b, ApJ 509, L109

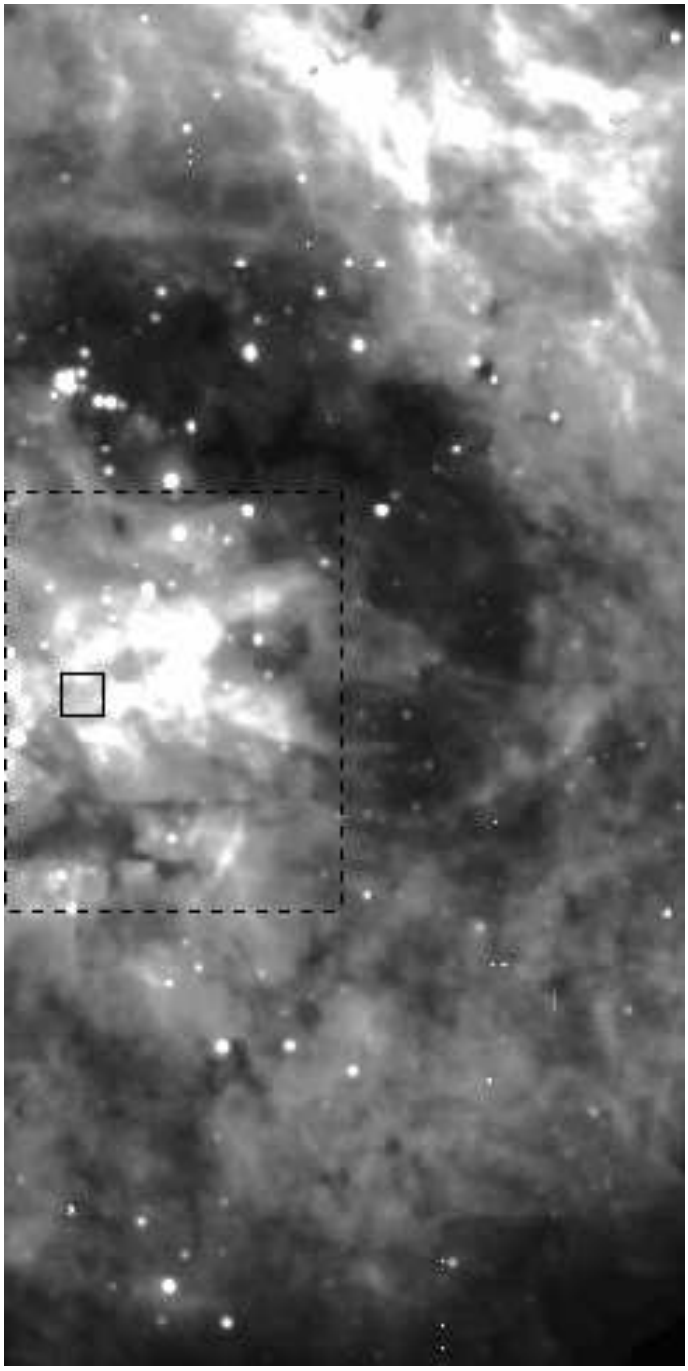

Fig. 1. SUSI2 H_α image of the 30 Doradus star forming region. The location of PSR J0537−6910 is near the center of the small $\simeq 20'' \times 20''$ solid square. The larger ($0\farcm5 \times 0\farcm5$) dashed box marks the area in which the search of stellar objects has been performed (see Sect. 2.2).

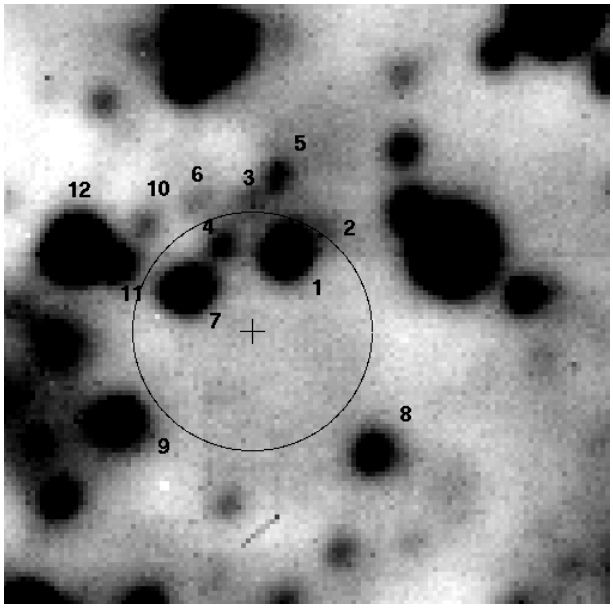

Fig. 2. $\simeq 20'' \times 20''$ I-band image of the PSR J0537−6910 surroundigs (North to the top, East to the left). The circle ($\simeq 4''$) marks the uncertainty region associated with the pulsar position as resulting from the combination of the error ($\simeq 3''$) on the boresight-corrected ROSAT/HRI coordinates (Wang & Gotthelf 1998b) and the global error budget of our astrometry. Objects detected close/inside the error circle are labelled 1–12.

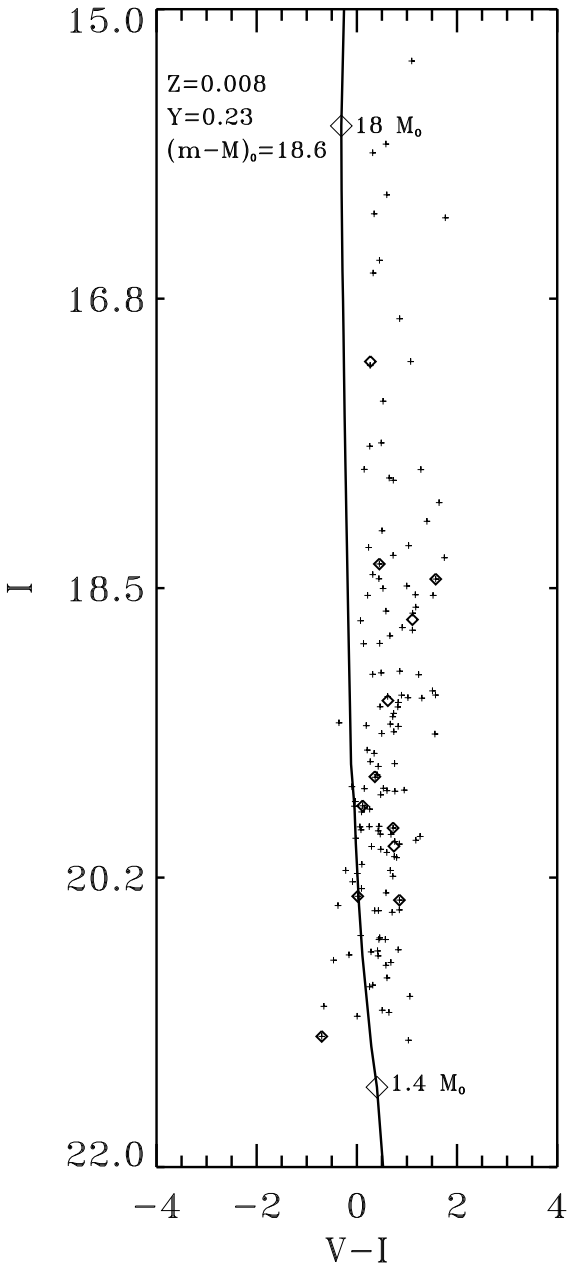

Fig. 3. Color–magnitude diagram of the objects found inside the dashed box in Fig. 1 (crosses) and the objects labelled in Fig. 2 (open diamonds). The solid line in the plot corresponds to the Zero Age Main Sequence computed for stars with a chemical composition $Z = 0.008, Y = 0.23$ and masses in the range from $m = 1.4 M_{\odot}$ to $m = 18 M_{\odot}$ (Cassisi, private comm.).